This article has been accepted for publication in a future issue of this journal, but has not been fully edited. Content may change prior to final publication. Citation information: DOI 10.1109/ACCESS.2018.2825371, IEEE Access

Accurate 3D Localization Method for Public Safety Applications in Vehicular Ad-hoc Networks

Abdul Rahim Ansari, *Student Member, IEEE*, Nasir Saeed, *Member, IEEE*, Mian Imtiaz Ul Haq and Sunghyun Cho *Member, IEEE*

***Abstract*—Vehicular ad hoc networks (VANETs) represent a very promising research area because of their ever increasing demand, especially for public safety applications. In VANETs vehicles communicate with each other to exchange road maps and traffic information. In many applications, location-based services are the main service, and localization accuracy is the main problem. VANETs also require accurate vehicle location information in real time. To fulfill this requirement, a number of algorithms have been proposed; however, the location accuracy required for public safety applications in VANETs has not been achieved. In this paper, an improved subspace algorithm is proposed for time of arrival (TOA) measurements in VANETs localization. The proposed method gives a closed-form solution and it is robust for large measurement noise, as it is based on the eigen form of a scalar product and dimensionality. Furthermore, we developed the Cramer-Rao Lower Bound (CRLB) to evaluate the performance of the proposed 3D VANETs localization method. The performance of the proposed method was evaluated by comparison with the CRLB and other localization algorithms available in the literature through numerous simulations. Simulation results show that the proposed 3D VANETs localization method is better than the literature methods especially for fewer anchors at road side units and large noise variance.**

***Index Terms*—Vehicular ad hoc networks (VANETs), Localization, Time of arrival (TOA), Cramer-Rao lower bound (CRLB)**

I. Introduction

Vehicular ad-hoc networks (VANETs) has become a remarkable research area for the automotive and communication industry. The driving force behind the innovations in VANETs is the advances in communication and information technology. In the past two decades, wireless communications have influenced our lifestyles such that everyone wants to be connected to the internet at any time and anywhere. Recently the concept of mobile connected vehicles is getting more attention, which leads to enable new areas of applications such as driver assistance, traffic flow, public safety, and infotainment [1]. Currently, most of the work on VANETs is to make the vehicles and roads capable to carry out secure transportation. The secure transportation means to provide the information about accidents, road conditions, weather conditions, traffic conditions and location-based services to the user [2], [3]. VANETs should also provide efficient transportation where efficient means short and predictable transportation time, reducing congestion and fuel saving [4], lower cost and better management of the public transport network [5]. VANETs can also collect and share the information about an area of interest [6] in different applications such as pollution control, public surveillance (photos taken of a violent act in progress) and traffic planning. VANETs will provide more enjoyable means to the user by giving access to the Internet, on road social media, tourist information, games and use of social applications [7].

VANETs is a special case of mobile ad-hoc network where vehicles are equipped with the capabilities of wireless communication and data processing. The direct communication from one vehicle to the other vehicle makes it possible to exchange information even without the communication infrastructure. The advances in wireless communications and user trends allow different deployment strategies for VANETs in rural and urban environments. The deployment of VANETs is to provide communication between vehicles and with the roadside units. There are three major possibilities for VANETs architecture as shown in Fig. 1.

- Vehicle to Infrastructure (V2I): This infrastructure allows the vehicle to communicate with the roadside units for data exchange and location-based services.
- Vehicle to Vehicle (V2V): It allows the vehicles to communicate directly with each other without the communication infrastructure. V2V is deployed

A. R. Ansari and S. Cho are with the Department of Computer Science and Engineering, Hanyang University, Ansan, Korea (e-mail: chopro@hanyang.ac.kr).

N. Saeed is with Department of Electrical Engineering, King Abdullah University of Science and Technology, Thuwal, Makkah, Saudi Arabia (e-mail: mr.nasir.saeed@ieee.org).

M. I. U. Haq is with Faculty of Electrical Engineering, University of Engineering and Technology, Peshawar, Pakistan (e-mail: imtiaz@uetpeshawar.edu.pk).

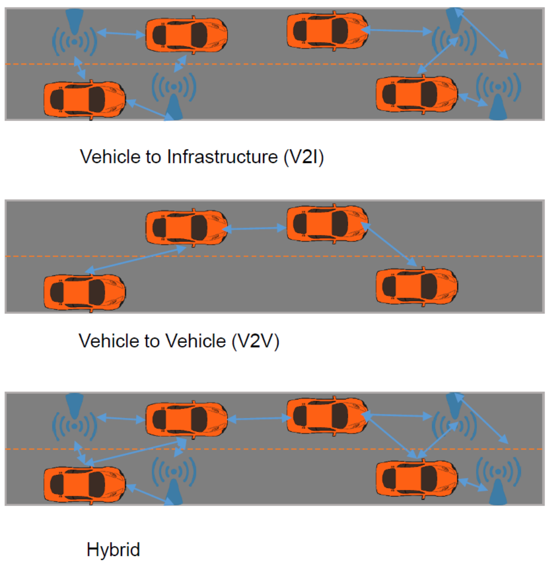

Fig. 1. Different deployment strategies for VANETs.

mainly for security and safety applications.

- Hybrid: It combines both V2V and V2I infrastructure to get benefit from both nearby vehicles and roadside units. This strategy enables long distance communication through multi-hop fashion.

In hybrid architecture of VANETs, vehicles can communicate with roadside units and with each other. VANETs is an important tool in traffic management systems. Recently, it has become the major element of intelligent transport systems. The goal of such systems is to provide a safe and pleasant journey to drivers and passengers. Safety applications are essential to vehicular to vehicular (V2V) communication as they can greatly reduce the chance of an accident. Public safety applications need real-time accurate vehicle position information. Therefore, it is important to accurately locate vehicles in VANETs.

Many methods have been proposed to meet the requirements of VANETs localization such as global positioning system (GPS) methods, geographical information system methods, cellular phone technology, and dead reckoning. However, these techniques have accuracy and reliability problems and they are not cost-effective. Besides cost, GPS signals are weak and can easily be blocked by different obstacles such as forests, buildings, etc. In the proposed method, the location of a vehicle is estimated by using anchor vehicles (AVs), i.e., vehicles which know their exact location. A few antennas are installed on roadside units, which act as AVs, as shown in Fig. 2. Location information can be updated regularly by allowing vehicles to share messages. These messages contain the time at which the message is sent, as this information is necessary for the time of arrival (TOA) method. The contributions of this paper are summarized as follows:

1) We propose a novel three-dimensional (3D) localization method for VANETs that allows us to accurately estimate the positions of multiple vehicles. The proposed method mainly relies on a subspace principle, but the co-variance matrix does not require any decomposition. Thus, the requirement of a pseudo-signal subspace vanishes, and we can avoid the main problem of eigen decomposition encountered in subspace methods.
2) The CRLB is analytically derived for the proposed algorithm, which gives a lower bound on the variance of an unbiased estimator [8].
3) The theoretical minimum square logarithmic error (MSLE) for the proposed algorithm is computed. Numerical results show that the proposed method outperforms several other popular localization algorithms. The effects of different system parameters such as measurement noise, density of AVs, and the number of simulations were investigated to evaluate the performance of the proposed algorithm.

Rest of the paper is organized as follows: Section II consists of related work, section III describes the system model. Proposed VANETs localization algorithm and its numerical results are described in section IV and V respectively. Finally the proposed work is concluded in section VI.

II. Related Work

Depending on the range measurement technique used, localization techniques can be subdivided into two main categories: the true range-based techniques and range-free techniques. Range-based techniques use range measurements calculated by each node to estimate location. However, connectivity information is used instead of true ranging for location estimation in range-free techniques. Ranging for localization is performed using different ranging techniques such as the received signal strength indicator (RSSI), the time difference of arrival (TDOA), the time of arrival (TOA) and the angle of arrival (AOA). In range-free approaches, locations of sensor nodes are estimated from simple connectivity information or the number of hops between each pair of sensor nodes [9]. RSSI computes the strength of the received signal, and the propagation loss is calculated based on RSSI. The RSSI technique is a cost-efficient solution for ranging as it does not require any extra hardware. However, its performance is often not satisfactory compared to other ranging techniques due to channel fading and

This article has been accepted for publication in a future issue of this journal, but has not been fully edited. Content may change prior to final publication. Citation information: DOI 10.1109/ACCESS.2018.2825371, IEEE Access

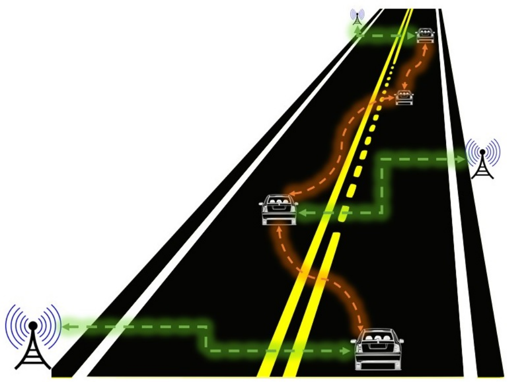

Fig. 2. System model.

multipath problems [10]. TOA measurement considers speed, wavelength and time for the radio signal to travel between two nodes [11]. The TDOA technique considers the time difference between two different kinds of signals arriving at the receiver. In the TDOA approach, the nodes need to be equipped with two kinds of extra devices, which can detect both kinds of signals. A receiver calculates the time difference between the two different signals and the distance information is estimated from the calculated time difference between the two nodes [12]. AOA ranging measurements are based on the angle of received signal at the receiver [13]. Usually TOA, TDOA and AOA are suitable for applications that require high accuracy, but they require more cost for the measurements.

Range-free techniques are regarded as a cost and energy efficient solution for locating nodes in wireless sensor networks. To find the actual coordinates of nodes without distance information, range-free techniques need a proper scaling factor because it strongly depends on hop count. Most of the range-free techniques compute the scaling from the ratio of the distance to the hop count [14] or based on the anchor locations [15]. Range-free schemes are easy to implement with low cost but these have the drawback of limited accuracy, particularly in practical applications [16]–[18].

In [19] the authors proposed a landscape 3D localization method with the help of mobile anchors. The main drawback of [19] is that the accuracy of their proposed method depends on the expensive mobile anchors. Range-free localization algorithms 3D DVHOP [20], 3D MDS-MAP [21] and 3D centroid are proposed in [22]. These range-free methods are complex as well as their localization accuracy is comparatively low. However, one method to increase the accuracy of 3D localization algorithm is to convert the cost function into a optimization problem. Particle swarm optimization algorithm, intelligent optimization algorithms e.g genetic algorithm and least squares support vector machine algorithm are applied in 3D space localization [23]–[25].

A number of localization methods for VANETs are introduced in [26] including cellular localization, image processing, relative localization, map matching and global positioning systems. In [27], the proposed localization method measures the inter-user radio distances using directional antennas, and then every user tries to locate itself with respect to the anchor node. In [28], the authors proposed a grid-based vehicle localization algorithm, which tries to minimize propagation error in the network by using the geometrical locations of the vehicles. In [28], the authors proposed that the grid-based schemes are less prone to error compared to non-grid based schemes. In [29], the authors proposed a VANETs localization scheme that strongly relies on road-side units. Every vehicle passing in the range of a road-side unit communicates with it through beacon signals and its position is estimated using TOA or TDOA measurements. In [30] and [31], the authors proposed cooperative vehicle localization in which different types of localization schemes were discussed for VANETs localization. The weighted localization method for VANETs was proposed in [32], where different weights have been assigned to the measurements based on the signal to interference noise ratio (SINR), where the closer vehicles have a high SINR and larger weights, while far away vehicles have a low SINR and smaller weights. In [33] the authors assume that vehicles have IEEE.802.11p interfaces, and the localization performance can be improved by combining vehicular communications and smartphone sensors.

III. System Model

A fully connected hybrid network is considered in our work, as this is the most frequently used assumption [34], [35]. To estimate the unknown vehicle (UV) position $\boldsymbol{\rho}_0 = [x_0, y_0, z_0]^T$ using a TOA ranging technique, we first assume that the AV's coordinates are $\{\boldsymbol{\rho}_k\}_{k=1}^{L}$, where $L \geqslant 4$ is the number of AVs in the VANETs. However, to obtain the unique position of the UV, the four AVs should not be coplanar with one another [36]. In [37], [38], mobility models for vehicles are classified into two major categories macroscopic and microscopic. Macroscopic models are based on fluid dynamics which considers the density of vehicles average velocity and vehicular traffic. Microscopic mobility models are more precise which consider every vehicle as a separate entity and modeling its nature. Microscopic models are more

This article has been accepted for publication in a future issue of this journal, but has not been fully edited. Content may change prior to final publication. Citation information: DOI 10.1109/ACCESS.2018.2825371, IEEE Access

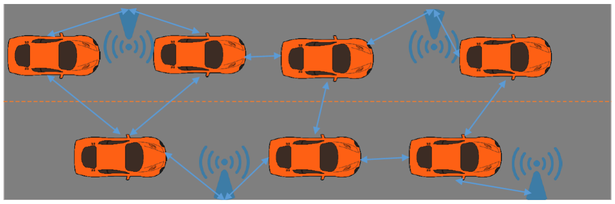

Fig. 3. An Overview of a Unidirectional Traffic Flow in VANETs

accurate but computationally more expensive. In this paper we considered a unidirectional urban traffic scenario where the vehicles are moving with low velocity. The vehicles that are added to the network follows Poisson Point Process (PPP) with intensity of λ, i.e. number of vehicles entering the network at time T. After the arrival of each vehicle i, it is assigned an independent uniformly distributed speed V_i, with probability distribution function of

$$f(V_i/s) = \frac{1}{\beta_m - \beta_n}, \qquad \beta_m > s > \beta_n, \tag{1}$$

where β_m is the maximum velocity and β_n is the minimum velocity of vehicle i. In unidirectional traffic flow where the vehicles coming into the range of AVs are localized whether the traffic flow is in a single lane or in two parallel lanes. Any vehicle i that is in the range of four AVs, is localized. Initially, we do not consider the direction of the vehicle at time instant T, but once the network is re-localized at time $\hat{T}$, the direction of the vehicle is also predicted. In order to clarify the scenario, Fig. 3 shows an overview of unidirectional VANETs, where the vehicles that come within the direct or multi-hop range of AVs (blue) are localized. Vehicles that are moving away from the transmission range of the network, become independent and further do not take any part in the formation of the network. In this paper, we have considered unit disk model for ranging. According to unit disk model, two vehicles can communicate with each other directly if and only if their Euclidean distance is less than their transmitting range. The actual distance between the UV and the kth AV is represented by

$$\zeta_{0k} = \|\boldsymbol{\rho}_0 - \boldsymbol{\rho}_k\|, \qquad k = 1, 2, ..., L. \tag{2}$$

The travel time by signal to move from the UV to the kth AV (in the absence of measurement noise) is denoted by t_{0k} and is given by

$$t_{0k} = \frac{\zeta_{0k}}{c}, \qquad k = 1, 2, ..., L. \tag{3}$$

Here, c is a constant i.e., the speed of light. Then, the TOA measurement can be written as [16]

$$\chi_{0k} = \zeta_{0k} + \omega_{0k}, \qquad k = 1, 2, ..., L, \tag{4}$$

where ω_{0k} is the additive zero mean white Gaussian having a variance of σ^2_{0k}, which is given by [39]

$$\sigma^2_{0k} = \varphi \zeta^{\nu}_{0k}, \tag{5}$$

where φ is a constant related to the AVs and ν is a path loss exponent. (4) can be written in vector form as

$$\boldsymbol{\chi} = \boldsymbol{\zeta} + \boldsymbol{\omega}, \tag{6}$$

where $\boldsymbol{\zeta} = [\zeta_{01}, ..., \zeta_{0L}]^T$ and $\boldsymbol{\omega} = [\omega_{01}, ..., \omega_{0L}]^T$.

IV. Proposed Algorithm

First, we define a $K \times 3$ matrix $\boldsymbol{\Lambda}$ i.e.,

$$\boldsymbol{\Lambda} = [\boldsymbol{\rho}_1 - \boldsymbol{\rho}_0, \boldsymbol{\rho}_2 - \boldsymbol{\rho}_0, ..., \boldsymbol{\rho}_L - \boldsymbol{\rho}_0]^T, \tag{7}$$

where $K = 3$ for 3D and $\boldsymbol{\Lambda}$ is parameterized by $\boldsymbol{\rho}_0$. The multidimensional similarity matrix can be defined as [40]

$$\boldsymbol{\Upsilon} = \boldsymbol{\Lambda}\boldsymbol{\Lambda}^T, \tag{8}$$

which is a positive semi-definite matrix [41], (m, n) and the value of $\boldsymbol{\Upsilon}$ is

$$[\Upsilon]_{mn} = \frac{(\zeta^2_{0m} - \zeta^2_{mn} + \zeta^2_{0n})}{2}, \tag{9}$$

where $\zeta_{mn} = \zeta_{nm} = \|\boldsymbol{\rho}_m - \boldsymbol{\rho}_n\|$ is the estimated distance between the mth UV and the nth AV. In fact, the exact value of $\boldsymbol{\Upsilon}$ is not available. But, at sufficiently low noise conditions, we can consider its approximate value represented by $\hat{\boldsymbol{\Upsilon}}$, with the use of estimated $\{\chi_{0m}\}$ and actual $\{\zeta_{mn}\}$ ranging measurements [40].

$$[\hat{\Upsilon}]_{mn} = \frac{(\chi^2_{0m} - \zeta^2_{mn} + \chi^2_{0n})}{2}. \tag{10}$$

We decompose the symmetric matrix $\hat{\boldsymbol{\Upsilon}}$ with the help of eigen decomposition to obtain [42]

$$\hat{\boldsymbol{\Upsilon}} = \boldsymbol{\Gamma}_{\mathfrak{s}}\boldsymbol{\Psi}_{\mathfrak{s}}\boldsymbol{\Gamma}^T_{\mathfrak{s}} + \boldsymbol{\Gamma}_{\mathfrak{n}}\boldsymbol{\Psi}_{\mathfrak{n}}\boldsymbol{\Gamma}^T_{\mathfrak{n}}, \tag{11}$$

where $\boldsymbol{\Psi}_{\mathfrak{s}}$=diag$(\lambda_1, \lambda_2, \lambda_3) \succ 0$, $\boldsymbol{\Psi}_{\mathfrak{n}}$=diag$(\lambda_4, \lambda_5, ..., \lambda_M)$ with $\lambda_4 = \lambda_5 = ... = \lambda_M = 0$ are the Eigenvalues of $\hat{\boldsymbol{\Upsilon}}$, and $\boldsymbol{\Gamma}_{\mathfrak{s}}$ and $\boldsymbol{\Gamma}_{\mathfrak{n}}$ are the Eigenvectors. Ideally, rank$(\boldsymbol{\Upsilon}) = 3$, we have

$$\hat{\boldsymbol{\Upsilon}} \quad = \boldsymbol{\Gamma}_{\mathfrak{s}}\boldsymbol{\Psi}_{\mathfrak{s}}\boldsymbol{\Gamma}^T_{\mathfrak{s}}, \tag{12}$$

which can also be re-written as

$$\boldsymbol{\Lambda}^p = \boldsymbol{\Gamma}_{\mathfrak{s}}\boldsymbol{\Psi}^{0.5}_{\mathfrak{s}}. \tag{13}$$

This article has been accepted for publication in a future issue of this journal, but has not been fully edited. Content may change prior to final publication. Citation information: DOI 10.1109/ACCESS.2018.2825371, IEEE Access

The relationship between the principle axis result and the actual global locations is

$$\mathbf{\Lambda} = \mathbf{\Lambda}^p \mathbf{\Omega}, \tag{14}$$

where $\mathbf{\Omega}$ is an unknown transformation that needs to be determined. The estimate of $\mathbf{\Omega}$ in the least square sense is [43]

$$\hat{\mathbf{\Omega}} = (\mathbf{\Lambda}^{pT}\mathbf{\Lambda}^p)^{-1}\mathbf{\Lambda}^{pT}\mathbf{\Lambda}. \tag{15}$$

However, it is not possible to calculate $\boldsymbol{\rho}_0$ from (14), as $\boldsymbol{\rho}_0$ is unknown in $\mathbf{\Lambda}$. Alternatively, (14) is simplified as

$$\mathbf{\Lambda} = \mathbf{\Gamma}_{\mathfrak{s}}\mathbf{\Gamma}_{\mathfrak{s}}^T\mathbf{\Lambda}. \tag{16}$$

by utilizing the property $\boldsymbol{I}_L - \mathbf{\Gamma}_{\mathfrak{s}}\mathbf{\Gamma}_{\mathfrak{s}}^T = \mathbf{\Gamma}_{\mathfrak{n}}\mathbf{\Gamma}_{\mathfrak{n}}^T$ [42], where $\boldsymbol{I}_L$ is the $L \times L$ identity matrix. Now (16) becomes

$$\mathbf{\Gamma}_{\mathfrak{n}}\mathbf{\Gamma}_{\mathfrak{n}}^T\mathbf{\Lambda} = \boldsymbol{\kappa}, \tag{17}$$

where $\boldsymbol{\kappa}$ represents a matrix with all zeros in the $L \times 3$ dimension. By re-arranging (17), we get

$$\mathbf{\Gamma}_{\mathfrak{n}}\mathbf{\Gamma}_{\mathfrak{n}}^T\varsigma_L\boldsymbol{\rho}_0^T \approx \mathbf{\Gamma}_{\mathfrak{n}}\mathbf{\Gamma}_{\mathfrak{n}}^T\mathbf{\Theta}, \tag{18}$$

where $\mathbf{\Theta} = [\boldsymbol{\rho}_1, \boldsymbol{\rho}_2, ..., \boldsymbol{\rho}_L]^T$ and ς_L is a column unity vector with a dimension of $L \times 1$. The final location estimation, i.e., the solution of (18), is given by

$$\hat{\boldsymbol{\rho}}_0 = \frac{\mathbf{\Theta}^T\mathbf{\Gamma}_{\mathfrak{n}}\mathbf{\Gamma}_{\mathfrak{n}}^T\varsigma_L}{\varsigma_L^T\mathbf{\Gamma}_{\mathfrak{n}}\mathbf{\Gamma}_{\mathfrak{n}}^T\varsigma_L}. \tag{19}$$

It is clear from (19)that the proposed solution does not need an a priori initial location estimation of the UV's, thus the proposed algorithm provides improved accuracy for UV localization in VANETs.

A. Analysis

The probability density function for χ_{0k}, conditioned on $\boldsymbol{\rho}_0$ and $\boldsymbol{\rho}_k$ can be written as

$$\mathfrak{f}(\chi_{0k}|\boldsymbol{\rho}_0, \boldsymbol{\rho}_k) = \frac{1}{\sqrt{2\pi\sigma_{0k}^2}} e^{\left(-\frac{1}{2\sigma_{0k}^2}(\chi_{0k}-\zeta_{0k})^2\right)}. \tag{20}$$

The likelihood ratio of (20) is then given by

$$\begin{aligned}\mathfrak{l}_{ij} = -0.5 \Bigg\{ & \log 2\pi\varphi + 0.5\nu\log(\|\boldsymbol{\rho}_0 - \boldsymbol{\rho}_k\|^2) \\ & + \frac{1}{\varphi}\frac{(\chi_{0k} - \|\boldsymbol{\rho}_0 - \boldsymbol{\rho}_k\|)^2}{(\|\boldsymbol{\rho}_0 - \boldsymbol{\rho}_k\|^2)^{\nu/2}} \Bigg\},\end{aligned} \tag{21}$$

and the joint log-likelihood is

$$\mathbf{\Phi}_{0k} = \sum_{k \in L} \log \mathfrak{f}(\chi_{0k}|\boldsymbol{\rho}_0, \boldsymbol{\rho}_k. \tag{22}$$

Now, putting (21) in (22), we get

$$\begin{aligned}\mathbf{\Phi}_{0k} = -0.5 \sum_{k \in L} \Bigg\{ & \log 2\pi\varphi + 0.5\nu\log(\|\boldsymbol{\rho}_0 - \boldsymbol{\rho}_k\|^2) \\ & + \frac{1}{\varphi}\frac{(\chi_{0k} - \|\boldsymbol{\rho}_0 - \boldsymbol{\rho}_k\|)^2}{(\|\boldsymbol{\rho}_0 - \boldsymbol{\rho}_k\|^2)^{\nu/2}} \Bigg\}.\end{aligned} \tag{23}$$

The CRLB sets a lower bound on the variance of any unbiased estimator. CRLB for $\boldsymbol{\rho}_0$ can be developed from a Fisher information matrix (FIM), $\mathbf{\Xi}(\boldsymbol{\rho}_0)$, [8], which is defined as

$$\mathbf{\Xi}(\boldsymbol{\rho}_0) = \mathbb{E}[-\triangle_{\boldsymbol{\rho}_0,\boldsymbol{\rho}_0}\mathbf{\Phi}_{0k}]. \tag{24}$$

Here, $\mathbb{E}$ and $\triangle_{\boldsymbol{\rho}_0,\boldsymbol{\rho}_0} \triangleq \nabla^T_{\boldsymbol{\rho}_0,\boldsymbol{\rho}_0}$ are the expected value and the second order derivative operators, respectively. $\mathbf{\Xi}(\boldsymbol{\rho}_0)$ in the form of submatrices can be written as

$$\mathbf{\Xi}(\boldsymbol{\rho}_0) = \begin{pmatrix} \Xi_{xx} & \Xi_{xy} & \Xi_{xz} \\ \Xi_{xy}^T & \Xi_{yy} & \Xi_{yz} \\ \Xi_{xz}^T & \Xi_{yz}^T & \Xi_{zz} \end{pmatrix}, \tag{25}$$

where subscripts xx, yy and zz in (25) indicate the diagonal elements, while, xy, xz and yz show the non-diagonal elements of $\mathbf{\Xi}(\boldsymbol{\rho}_0)$. Each element of $\mathbf{\Xi}(\boldsymbol{\rho}_0)$ is given by

$$\Xi_{xx} = \sum_{k \in L} \frac{1}{\sigma_{0k}^2}\frac{\vartheta_{0k}(x_0 - x_k)^2}{\|\boldsymbol{\rho}_0 - \boldsymbol{\rho}_k\|^2}, \tag{26a}$$

$$\Xi_{xy} = \sum_{k \in L} \frac{1}{\sigma_{0k}^2}\frac{\vartheta_{0k}(x_0 - x_k)(y_0 - y_k)}{\|\boldsymbol{\rho}_0 - \boldsymbol{\rho}_k\|^2}, \tag{26b}$$

$$\Xi_{xz} = \sum_{k \in L} \frac{1}{\sigma_{0k}^2}\frac{\vartheta_{0k}(x_0 - x_k)(z_0 - z_k)}{\|\boldsymbol{\rho}_0 - \boldsymbol{\rho}_k\|^2}, \tag{26c}$$

$$\Xi_{yy} = \sum_{k \in L} \frac{1}{\sigma_{0k}^2}\frac{\vartheta_{0k}(y_0 - y_k)^2}{\|\boldsymbol{\rho}_0 - \boldsymbol{\rho}_k\|^2}, \tag{26d}$$

$$\Xi_{yz} = \sum_{k \in L} \frac{1}{\sigma_{0k}^2}\frac{\vartheta_{0k}(y_0 - y_k)(z_0 - z_k)}{\|\boldsymbol{\rho}_0 - \boldsymbol{\rho}_k\|^2}, \tag{26e}$$

$$\Xi_{zz} = \sum_{k \in L} \frac{1}{\sigma_{0k}^2}\frac{\vartheta_{0k}(z_0 - z_k)^2}{\|\boldsymbol{\rho}_0 - \boldsymbol{\rho}_k\|^2}, \tag{26f}$$

where $\vartheta_{0k} = 1 + 0.5\nu^2\varphi\zeta_{0k}^{\nu-2}$ is the scaling factor, which depends on distance . The CRLB$(\boldsymbol{\rho}_0)$ is given by [8]

$$\begin{aligned}\text{CLB}(\boldsymbol{\rho}_0) \quad = \quad & [\mathbf{\Xi}^{-1}(\boldsymbol{\rho}_0)]_{1,1} + [\mathbf{\Xi}^{-1}(\boldsymbol{\rho}_0)]_{2,2} \\ & + [\mathbf{\Xi}^{-1}(\boldsymbol{\rho}_0)]_{3,3}.\end{aligned} \tag{27}$$

This article has been accepted for publication in a future issue of this journal, but has not been fully edited. Content may change prior to final publication. Citation information: DOI 10.1109/ACCESS.2018.2825371, IEEE Access

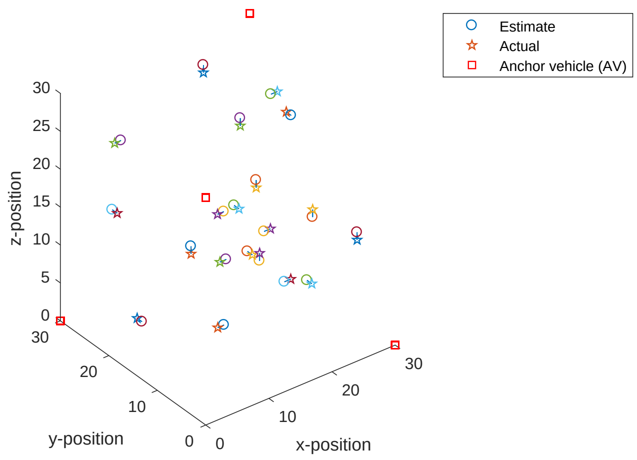

Fig. 4. Localization of UVs in 3D with 20 UVs.

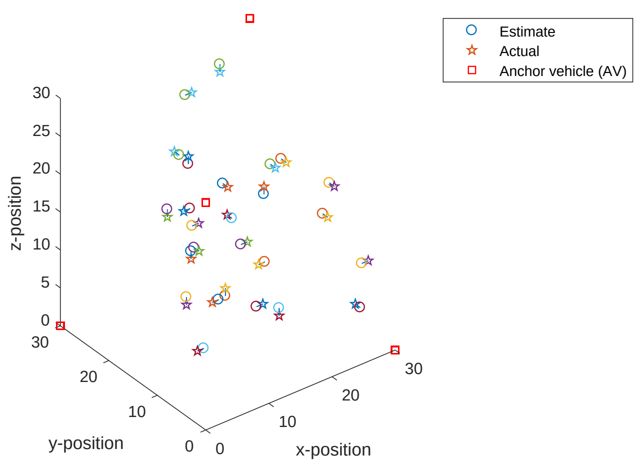

Fig. 5. Localization of UVs in 3D with 25 UVs.

Finally, the CRLB for the proposed algorithm is

$$\sqrt{\Pi} \geq \text{CRLB}, \tag{28}$$

where MSLE (Π) is

$$\Pi = \mathbb{E}[(\hat{\boldsymbol{\rho}}_0 - \boldsymbol{\rho}_0)^T(\hat{\boldsymbol{\rho}}_0 - \boldsymbol{\rho}_0)], \tag{29}$$

$\boldsymbol{\rho}_0$ and $\hat{\boldsymbol{\rho}}_0$ are the actual and estimated positions of UV, respectively.

V. Numerical Examples

A. Simulation Setup

Numerous simulations were performed to analyze the proposed localization algorithm performance by comparing it with the existing literature [18], [26], [28] and CRLB. The following parameters are taken for simulation purposes. A $30 \times 30 \times 30\ m^3$ volume was assumed.

TABLE I
Simulation Parameters

Parameter	Values
Volume	$30 \times\ 30\ \times\ 30\ m^3$
Number of UVs	20-25
Number of AVs	4-9
Variance	10-50
Velocity	$5\ m/s$

20 UVs were generated randomly moving with velocity of $5\ m/s$ and 4 AVs at $[30;0;0]^T$, $[0;30;0]^T$, $[0;0;30]^T$ and $[30;30;30]^T$ locations were considered. The ranging error ω_{0K} was a zero-mean white Gaussian process having a variance of σ^2_{0K}. The simulation parameters are given in Table I.

B. Monte Carlo Simulations

The following four different setups were simulated to evaluate the performance of the method.

- Setup 1: This is the same setup as described in Section V-A, such that the locations of the AVs form a convex hull around 20 UVs at time instant $t = t_1$. Fig. 4 illustrates this setup for the given simulation scenario, where the circles show the actual location of UVs, stars represent the estimated locations and squares show the location of AVs. We assumed that all UVs are moving at constant speed i.e, $5\ m/s$. After a certain time, i.e., at time instant $t = t_2$, 5 more UVs join the network as shown in Fig. 5. As the number of UVs is increased from 20 to 25 the MSLE of the network also increases because the 5 new UVs have extra localization error.
- Setup 2a: In this setup, the impact of fewer Monte Carlo simulations on MSLE was studied. However, the UV and AV configurations are the same as discussed in Setup 1. The range error variance was kept in the range of $10 - 50$ dBm^2. It is clear from Fig. 6 that the proposed technique outperforms the literature, but there are some fluctuations in the MSLE due to a smaller number of Monte Carlo simulations. Noted that for the proposed localization method each simulation generates independent and identically distributed results. Therefore the variance of MSLE is modeled as Bernoulli trail $p(1-p)/n \leq 1/4n$, where p is the true probability and n is the number of Monte Carlo simulations. The variance of the simulation results shrinks with an increase in the number of simulations. Generally, in order to investigate the properties of a localization estimator, the number of simulations is chosen

This article has been accepted for publication in a future issue of this journal, but has not been fully edited. Content may change prior to final publication. Citation information: DOI 10.1109/ACCESS.2018.2825371, IEEE Access

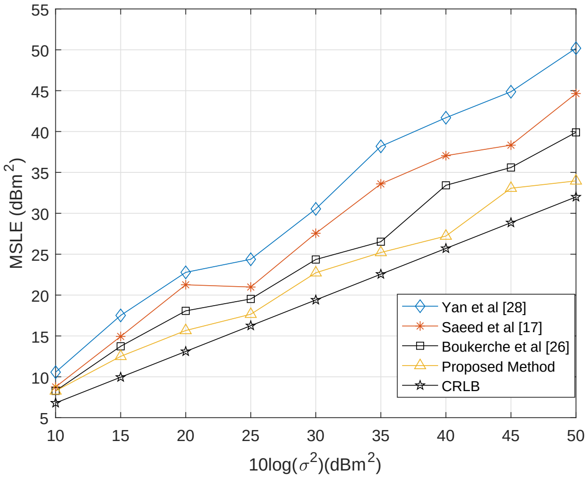

Fig. 6. MSLE performance vs range error variance in VANETs with 20 runs.

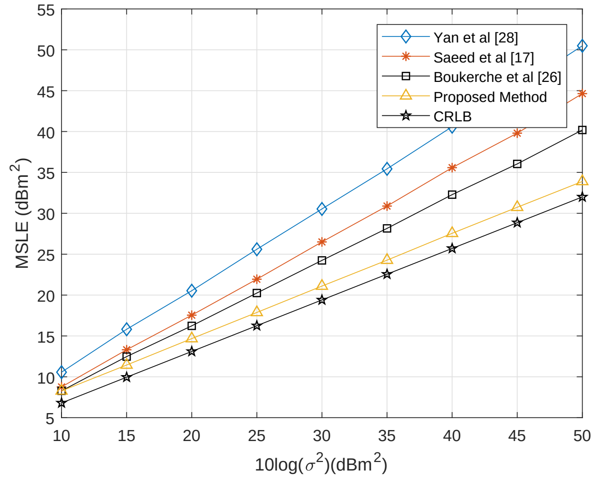

Fig. 7. MSLE performance vs range error variance in VANETs with 5000 runs.

to achieve a certain accuracy. It is shown in Fig. 6 that for a small value of n there is large error variance in the results. In the next setup, we show that increasing the value of n improves the results by reducing the fluctuations.

- Setup 2b: In this scenario, the number of Monte Carlo simulations n is increased from 20 to 5000. However, vehicle geometries (i.e., AVs and UVs) are the same as in Setup 1. It is clear from Fig. 7 that the proposed algorithm is less sensitive to noise than the literature for a high ranging error. Specifically, the proposed algorithm achieves about 30.76%-79.67% improvement in terms of MSLE. Moreover, Fig. 7 shows that the proposed method can reach the CRLB with a low range error variance. Furthermore, the irregularity that was present in Fig. 6 was also removed by increasing the number of Monte Carlo simulations.
- Setup 3: In this setup, the geometry of vehicles in a network (i.e., AVs and UVs) remained the same as discussed in Setup 1. The effect of additional AVs on the performance of the proposed algorithm is shown in Fig. 8. Here range error variance is assumed to be 20 dBm^2. As the number of AVs increased in the network, the localization error was reduced. Due to the fact that in this case, each UV has the reference information from more AVs. It is also shown in Fig. 8 that the performance of each algorithm is improved when AVs are increased from 4 to 9, but increasing the AVs further from 9 does not improve the localization performance because the network is saturated with anchors. Thus, from Fig. 8 the optimal number of AVs can be chosen for a specific scenario.

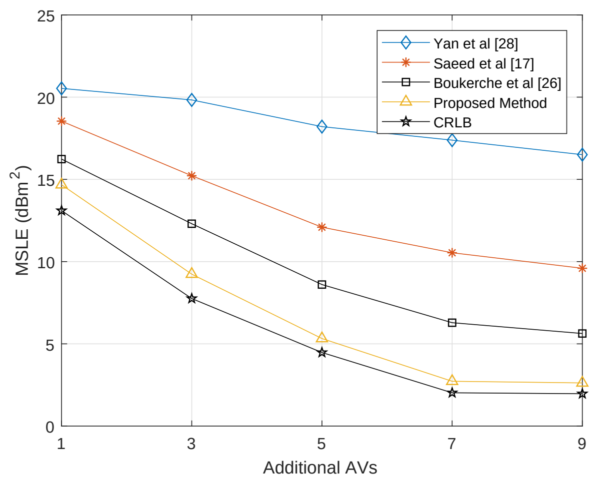

Fig. 8. MSLE performance vs number of additional AVs in VANETs.

VI. Conclusion

In this paper, we proposed an accurate localization algorithm for public safety applications for vehicular ad-hoc networks (VANETs) with time of arrival (TOA) measurements. Cramer Rao lower bound (CRLB) is also derived for the proposed VANETs localization algorithm because CRLB is the benchmark to evaluate the performance of any localization algorithm. Furthermore, numerous simulations are conducted to investigate the performance of the proposed algorithm. The simulations showed that the performance of the proposed algorithm is better than those in the literature especially for fewer anchor vehicles (AVs) and at a high noise variance. Future work will focus on improving the mean square localization error (MSLE) of the proposed method by changing the value of ζ_{0k}, although values of σ_{0k}^2 remain the same in a rank reduction method or by obtaining a better estimate of $\mathbf{\Lambda}$ from $\hat{\mathbf{\Upsilon}}$ by utilizing a proper weighting matrix.

VII. Acknowledgement

This work was supported by Basic Science Research Program through the National Research Foundation of Korea (NRF) funded by the Ministry of Education (No. NRF-2015R1D1A1A01059473).

References

[1] F. Cunha, L. Villas, A. Boukerche, G. Maia, A. Viana, R. A. Mini, and A. A. Loureiro, “Data communication in vanets,” *Ad Hoc Netw.*, vol. 44, no. C, pp. 90–103, Jul. 2016.

[2] N. M. Chowdhury, L. Mackenzie, and C. Perkins, “Requirement analysis for building practical accident warning systems based on vehicular ad-hoc networks,” in *Annual Conference on Wireless On-demand Network Systems and Services (WONS)*, Apr. 2014, pp. 81–88.

[3] M. Noussaiba and R. Rahal, “State of the art: Vanets applications and their rfid-based systems,” in *International Conference on Control, Decision and Information Technologies (CoDIT)*, Apr. 2017, pp. 0516–0520.

[4] P. Y. Chen, J. W. Liu, and W. T. Chen, “A fuel-saving and pollution-reducing dynamic taxi-sharing protocol in vanets,” in *72nd Vehicular Technology Conference - Fall*, Sep. 2010, pp. 1–5.

[5] R. P. Loce, R. Bala, and M. Trivedi, *Traffic Flow Analysis*. Wiley-IEEE Press, 2017, pp. 432–470.

[6] Q. Yan, M. Li, Z. Yang, W. Lou, and H. Zhai, “Throughput analysis of cooperative mobile content distribution in vehicular network using symbol level network coding,” *IEEE J. Sel. Areas Commun.*, vol. 30, no. 2, pp. 484–492, Feb 2012.

[7] J. Contreras, S. Zeadally, and J. A. Guerrero-Ibanez, “Internet of vehicles: Architecture, protocols, and security,” *IEEE IoT J.*, vol. 2, no. 9, pp. 1–10, Apr 2017.

[8] S. M. Kay, *Fundamentals of Statistical Signal Processing: Estimation Theory*. Prentice-Hall, Inc., 1993.

[9] J. M. Cabero, I. Olabarrieta, S. G. López, J. D. Ser, and J. L. Martín, “Range-free localization algorithm based on connectivity and motion,” *Springer Journal of Wireless Networks*, pp. 1–19, May 2014.

[10] G. Wang and K. Yang, “A new approach to sensor node localization using RSS measurements in wireless sensor networks,” *IEEE Trans. Wireless Commun.*, vol. 10, no. 5, pp. 1389–1395, May 2011.

[11] J. Y. Lee and R. A. Scholtz, “Ranging in a dense multipath environment using an UWB radio link,” *IEEE J. Sel. Areas Commun.*, vol. 20, no. 9, pp. 1677–1683, Dec. 2002.

[12] S. Hara, D. Anzai, T. Yabu, K. Lee, T. Derham, and R. Zemek, “A perturbation analysis on the performance of TOA and TDOA localization in mixed LOS/NLOS environments,” *IEEE Trans. Commun.*, vol. 61, no. 2, pp. 679–689, Feb. 2013.

[13] H. J. Shao, X. P. Zhang, and Z. Wang, “Efficient closed-form algorithms for AOA based self-localization of sensor nodes using auxiliary variables,” *IEEE Trans. Signal Process.*, vol. 62, no. 10, pp. 2580–2594, May 2014.

[14] D. Niculescu and B. Nath, “DV based positioning in ad hoc networks,” *J. Telecommun. Syst.*, vol. 22, pp. 265–280, Jan. 2003.

[15] Y. Shang, W. Ruml, Y. Zhang, and M. Fromherz, “Localization from mere connectivity,” in *Proc. ACM Mobihoc, Annapolis, MD*, Jun. 2003, pp. 201–212.

[16] M. I. ul Haq and D. Kim, “A novel localization algorithm for internet of things in 3d,” in *International Conference on Information and Communication Technology Convergence (ICTC)*, Oct. 2015, pp. 237–241.

[17] N. Saeed and H. Nam, “MDS-LM for wireless sensor networks localization,” in *IEEE 79th Vehicular Technology Conference*, May 2014, pp. 1–6.

[18] ——, “Robust multidimensional scaling for cognitive radio network localization,” *IEEE Trans. Veh. Technol.*, vol. 64, no. 9, pp. 4056–4062, Sep. 2015.

[19] L. Zhang, X. Zhou, and Q. Cheng, “Landscape-3D; a robust localization scheme for sensor networks over complex 3d terrains,” in *31st IEEE Conference on Local Computer Networks*, Nov. 2006, pp. 239–246.

[20] T. He, C. Huang, B. M. Blum, J. A. Stankovic, and T. Abdelzaher, “Range-free localization schemes for large scale sensor networks,” in *Proceedings of the 9th Annual International Conference on Mobile Computing and Networking*, ser. MobiCom. ACM, 2003, pp. 81–95.

[21] G. Tan, H. Jiang, S. Zhang, and A.-M. Kermarrec, “Connectivity-based and anchor-free localization in large-scale 2d/3d sensor networks,” in *Proceedings of the Eleventh ACM International Symposium on Mobile Ad Hoc Networking and Computing*. ACM, 2010, pp. 191–200.

[22] N. Bulusu, J. Heidemann, and D. Estrin, “GPS-less low-cost outdoor localization for very small devices,” *IEEE Personal Communications*, vol. 7, no. 5, pp. 28–34, Oct. 2000.

[23] A. Gopakumar and L. Jacob, “Localization in wireless sensor networks using particle swarm optimization,” in *IET International Conference on Wireless, Mobile and Multimedia Networks*, Jan. 2008, pp. 227–230.

[24] A. Kumar, A. Khosla, J. S. Saini, and S. Singh, “Stochastic algorithms for 3d node localization in anisotropic wireless sensor networks,” in *Proceedings of Seventh International Conference on Bio-Inspired Computing: Theories and Applications (BIC-TA)*, vol. 1, 2012, p. 1.

[25] Z. Cheng-lin, W. Xiong-lie, S. Xue-bin, and J. Ting, “A 3d wsn localization method based on particle swarm optimization algorithm,” *Journal of China Academy of Electronics and Information Technology*, vol. 1, p. 019, 2011.

[26] A. Boukerche, H. A. Oliveira, E. F. Nakamura, and A. A. Loureiro, “Vehicular ad hoc networks: A new challenge for localization-based systems,” *Computer Communications*, vol. 31, no. 12, pp. 2838 – 2849, 2008.

[27] H. Akcan and C. Evrendilek, “GPS-free directional localization via dual wireless radios,” *Computer Communications*, vol. 35, no. 9, pp. 1151 – 1163, 2012.

[28] T. Yan, W. Zhang, and G. Wang, “A grid-based on-road localization system in VANET with linear error propagation,” *IEEE Trans. Wireless Commun.*, vol. 13, no. 2, pp. 861–875, Feb. 2014.

[29] C.-H. Ou, “A roadside unit-based localization scheme for vehicular ad hoc networks,” *International Journal of Communication Systems*, vol. 27, no. 1, pp. 135–150, 2014.

[30] M. Obst, N. Mattern, R. Schubert, and G. Wanielik, “Car-to-car communication for accurate vehicle localization; the covel approach,” in *International Multi-Conference on Systems, Signals and Devices (SSD)*, Mar. 2012, pp. 1–6.

[31] N. Mattern, M. Obst, R. Schubert, and G. Wanielik, “Co-operative vehicle localization algorithm; evaluation of the covel approach,” in *International Multi-Conference on Systems, Signals and Devices (SSD)*, Mar. 2012, pp. 1–5.

This article has been accepted for publication in a future issue of this journal, but has not been fully edited. Content may change prior to final publication. Citation information: DOI 10.1109/ACCESS.2018.2825371, IEEE Access

[32] L. Altoaimy, I. Mahgoub, and M. Rathod, "Weighted localization in vehicular ad hoc networks using vehicle-to-vehicle communication," in *Global Information Infrastructure and Networking Symposium (GIIS)*, Sep. 2014, pp. 1–5.

[33] S. B. Cruz, T. E. Abrudan, Z. Xiao, N. Trigoni, and J. Barros, "Neighbor-aided localization in vehicular networks," *IEEE Trans. on Intell. Transport. Sys.*, vol. PP, no. 99, pp. 1–10, Feb. 2017.

[34] Y. Shang, W. Rumi, Y. Zhang, and M. Fromherz, "Localization from connectivity in sensor networks," *IEEE Trans. Parallel Distrib. Syst.*, vol. 15, no. 11, pp. 961–974, Nov. 2004.

[35] X. Ji and H. Zha, "Robust sensor localization algorithm in wireless ad-hoc sensor networks," in *Proc. 12th Inl. IEEE Conf. Comp. Commun. and Networks*, Oct. 2003, pp. 527–532.

[36] M. Mortenson, *Geometric Transformations For 3D Modeling*, 2nd ed. Industrial Press, Inc., 1995.

[37] J. Harri, F. Filali, and C. Bonnet, "Mobility models for vehicular ad hoc networks: a survey and taxonomy," *IEEE Commun. Surveys Tuts.*, vol. 11, no. 4, pp. 19–41, Dec. 2009.

[38] T. Umer, M. Amjad, N. Shah, and Z. Ding, *Modeling Vehicles Mobility for Connectivity Analysis in VANET*. Cham: Springer International Publishing, 2016, pp. 221–239.

[39] J. Xu, M. Ma, and C. Law, "Performance of time-difference-of-arrival ultra wideband indoor localisation," *IET Sci., Meas. Technol*, vol. 5, no. 2, pp. 46–53, Mar. 2011.

[40] Q. Wan, Y.-J. Luo, W.-L. Yang, J. Xu, J. Tang, and Y.-N. Peng, "Mobile localization method based on multidimensional similarity analysis," in *Proc. IEEE Int. Conf. Acoust., Speech, Signal Processing*, vol. 4, Mar. 2005, pp. 1081–1084.

[41] G. H. Golub and C. F. Van Loan, *Matrix Computations*. JHU Press, 2012.

[42] V. D. Veen, A. Jan, and E. D. Deprettere, "Subspace-based signal analysis using singular value decomposition," *Proc. IEEE*, vol. 81, no. 9, pp. 1277–1308, 1993.

[43] C. Lawson and R. Hanson, *Solving Least Squares Problems*. SIAM, 1995.